Mineralogical Magazine (2022), **86**, 340–345
doi:10.1180/mgm.2022.28

CAMBRIDGE UNIVERSITY PRESS

Article

Ferrofettelite, $[Ag_6As_2S_7][Ag_{10}FeAs_2S_8]$, a new sulfosalt from the Glasberg quarry, Odenwald, Germany

Luca Bindi[1,2*] and Robert T. Downs[3]

[1]Dipartimento di Scienze della Terra, Università degli Studi di Firenze, Via G. La Pira, 4 – I-50121 Firenze, Italy; [2]CNR-Istituto di Geoscienze e Georisorse, Sez. di Firenze, Via G. La Pira, 4 – I-50121 Firenze, Italy; and [3]Department of Geosciences, University of Arizona, Tucson, Arizona, 85721-0077, USA

Abstract

Ferrofettelite, ideally $[Ag_6As_2S_7][Ag_{10}FeAs_2S_8]$, is a new mineral (IMA2021-094) from the Glasberg quarry, Nieder-Beerbach, Odenwald, south-western Germany. It occurs as anhedral to subhedral flakes and grains up to 80 μm, associated with proustite and xanthoconite, on arsenolite, calcite and prehnite. Ferrofettelite is opaque with a metallic lustre and possesses a dark reddish-grey streak. It is brittle with an uneven fracture; the Vickers microhardness (VHN_{20}) is 122 kg/mm^2 (range 111–131). The calculated density is 5.74 g/cm^3 (on the basis of the empirical formula). In plane-polarised reflected light, ferrofettelite is greyish white. Between crossed polars it is weakly anisotropic with red internal reflections. Electron-microprobe analyses give the chemical formula $Ag_{16.04}(Fe_{0.55}Hg_{0.40}Cu_{0.02})_{\Sigma 0.97}(As_{3.94}Sb_{0.03})_{\Sigma 3.97}S_{15.02}$ on the basis of total atoms = 36.

Ferrofettelite is monoclinic, space group $C2$, with $a = 26.011(2)$, $b = 15.048(1)$, $c = 15.513(1)$ Å, $\beta = 90.40(1)°$ and $V = 6071.9(7)$ Å^3 for $Z = 8$. The six strongest Bragg peaks in the powder X-ray diffraction pattern (*d*, Å (*I*, %) (*hkl*) are: 3.18 (50) ($\bar{8}01$), 3.104 (100) (005), 3.004 (60) ($\bar{8}02$), 2.755 (40) ($\bar{4}43$), 2.501 (30) ($\bar{4}44$) and 1.880 (30) ($\bar{12}40$). The crystal structure can be described as the alternation of two kinds of layers along the **c**-axis: layer *A* with general composition $[Ag_6As_2S_7]^{2-}$ and layer *B* with a general composition of $[Ag_{10}FeAs_2S_8]^{2+}$. In the structure, the Ag atoms adopt various coordinations extending from quasi linear to quasi tetrahedral, the AsS_3 groups form pyramids as are typically observed in sulfosalts, and mixed (Fe,Hg) links two sulfur atoms in a linear coordination. Ferrofettelite is the first reported inorganic phase showing a linear coordination for Fe^{2+}. The high-temperature behaviour of ferrofettelite was studied up to 410 K and compared to that of fettelite.

Keywords: fettelite, Hg-sulfosalts, pearceite, polybasite, crystal structure, linear coordination, high temperature, Glasberg quarry, Odenwald, Germany

(Received 31 January 2022; accepted 14 March 2022; Accepted Manuscript published online: 25 March 2022; Associate Editor: Sergey V Krivovichev)

Introduction

To confirm that the revised chemical formula for fettelite from Chañarcillo, Chile, $[Ag_6As_2S_7][Ag_{10}HgAs_2S_8]$, proposed by Bindi *et al.* (2009) is valid for all the fettelite samples, and to elucidate the role of the cation substitution at the linearly-coordinated Hg site, Bindi *et al.* (2012) reported a structural and chemical characterisation of two samples of fettelite from the type locality (Glasberg quarry, Nieder-Beerbach, Odenwald, south-western Germany). One of these samples turned out to be a possible new Fe-rich end-member. However, Bindi *et al.* (2012) obtained a chemical composition significantly different from ideal [i.e. ΣS = 15 atoms per formula unit, Σ(As+Sb) = 4 apfu, Ag = 16 apfu] owing to the strong sensitivity of these samples to the electron beam that made it very difficult to attain good and reliable microprobe data. Recently, with new equipment and standards, the problem was solved, and good chemical data were obtained. This allowed us to go ahead with the submission of a new mineral proposal. The mineral and name was approved by the Commission on New Minerals, Nomenclature and Classification of the International Mineralogical Association (IMA2021–094, Bindi and Downs, 2022) as ferrofettelite (symbol Fftt). The name indicates that the mineral is the Fe-dominant analogue of fettelite. Holotype material is deposited in the collections of the University of Arizona Gem and Mineral Museum, Tucson, Arizona, USA, catalogue number 22716.

Occurrence, physical and optical properties

The sample containing ferrofettelite was not found *in situ*, but originates from a sample (Fig. 1), which belonged to the William W. Pinch collection, reported to come from the Glasberg quarry, Nieder-Beerbach, Odenwald, south-western Germany (the type locality of fettelite; Wang and Paniagua, 1996). Associated minerals include proustite and xanthoconite, on arsenolite, calcite and prehnite. We note that the association of fettelite with arsenolite was not reported by Wang and Paniagua (1996). As reported by Bindi *et al.* (2012), ferrofettelite, up to 250 μm in size, shows a grey reddish streak; it is opaque in transmitted light and exhibits a metallic lustre. No cleavage is observed, and the fracture is uneven. The calculated density (for

*Author for correspondence: Luca Bindi, Email: luca.bindi@unifi.it
Cite this article: Bindi L. and Downs R.T. (2022) Ferrofettelite, $[Ag_6As_2S_7][Ag_{10}FeAs_2S_8]$, a new sulfosalt from the Glasberg quarry, Odenwald, Germany. *Mineralogical Magazine* **86**, 340–345. https://doi.org/10.1180/mgm.2022.28

Fig. 1. Macroscopic image of the rock sample containing ferrofettelite (dark red). Scale bar and sample number are indicated.

$Z = 8$) from the empirical formula and single-crystal X-ray data is 5.74 g/cm^3. Micro-indentation measurements carried out with a VHN load of 20 g give a mean value of 122 kg/mm^2 (range: 111–131). A REE-super-magnet was placed in close proximity to a 200 µm fragment of ferrofettelite to explore potential paramagnetic susceptibility, but no effect was observed.

In plane-polarised incident light, ferrofettelite is greyish white in colour, with moderate bireflectance (from white to brownish grey). Under crossed polars, it shows weak anisotropism with relatively strong red internal reflections. Reflectance measurements were performed in air by means of a MPM-200 Zeiss microphotometer equipped with a MSP-20 system processor on a Zeiss Axioplan ore microscope. The filament temperature was ~3350 K. An interference filter was adjusted to four wavelengths for measurement (471.1, 548.3, 586.6 and 652.3 nm). Readings were taken for the specimen and standard (SiC) at the same focus conditions. The diameter of the circular area that was measured was 0.1 mm. Reflectance percentages for R_{min} and R_{max} are 28.2, 29.4 (471.1 nm); 25.0, 26.3 (548.3 nm); 22.9, 23.5 (586.6 nm); and 20.9, 21.2 (652.3 nm).

Chemical composition

The chemical composition was determined using wavelength dispersive analysis (WDS) by means of a JEOL 8200 electron microprobe. Concentrations of major and minor elements were determined at an accelerating voltage of 15 kV and a beam current of 15 nA, with 20 s counting time (spot size 1 µm). For the WDS analyses the following lines were used: S*Kα*, Fe*Kα*, Cu*Kα*, As*Lα*, Ag*Lα*, Sb*Lβ*, Pb*Mα* and Hg*Lα*. The standards employed were: pure metals for Cu and Ag, galena for Pb, pyrite for Fe and S, cinnabar for Hg, synthetic Sb_2S_3 for Sb and synthetic As_2S_3 for As. The ferrofettelite fragment was homogeneous within analytical error ($N = 4$).

It is noted that Bindi *et al.* (2012) previously reported a chemical analysis of ferrofettelite from the same specimen. They obtained a chemical composition significantly different from ideal, i.e. $Ag_{16.45}(Fe_{0.89}Hg_{0.37}Cu_{0.01})_{\Sigma 1.27}(As_{4.03}Sb_{0.04})_{\Sigma 4.07}S_{14.21}$. These authors discussed the strong sensitivity of these samples to the electron beam, which caused Hg to vaporise out of the sample (they observed a gradual reduction of Hg with time and significant damage to the sample surface). This made it very difficult to obtain good and reliable microprobe data. Here, with new equipment (JEOL-JXA8600 vs. JEOL-JXA8320) and standards (same kind of materials but newly prepared with vibro-

Table 1. Analytical data (in wt.%) for ferrofettelite.

Constituent	Mean	Range	S.D.	Probe standard
Ag	65.66	65.12–66.14	0.87	Ag-metal
Cu	0.05	0.02–0.09	0.02	Cu-metal
Pb	0.01	0.00–0.05	0.02	galena
Fe	1.16	0.99–1.25	0.06	pyrite
Hg	3.04	2.90–3.17	0.08	cinnabar
As	11.21	11.02–11.34	0.26	synthetic As_2S_3
Sb	0.14	0.11–0.20	0.05	synthetic Sb_2S_3
S	18.27	18.11–18.40	0.39	pyrite
Total	99.43	99.20–100.02		

S.D. = standard deviation

Table 2. Observed and calculated powder X-ray diffraction data (d in Å) for ferrofettelite.

1		2		
d_{obs}	I_{est}	d_{calc}	I_{calc}	*hkl*
-	**-**	7.7563	14	002
6.0	10	5.9974	10	221
-	-	4.9962	7	$\bar{2}21$
-	-	3.7562	4	620
3.26	10	3.2563	16	440
3.18	**50**	3.2513, 3.1866	8, 23	800, $\bar{8}01$
-	-	3.1846	39	441
3.104	**100**	3.1025	100	005
3.004	**60**	3.0060	21	$\bar{8}02$
2.930	15	2.9987, 2.9343	43, 9	442, $\bar{8}21$
-	-	2.9273	8	821
-	-	2.8413	6	640
-	-	2.7915	4	$\bar{8}22$
2.755	**40**	2.7598	32	$\bar{4}43$
-	**-**	2.7511	8	443
-	**-**	2.7438	15	803
-	**-**	2.6719	7	$\bar{6}42$
2.501	**30**	2.4981	28	$\bar{4}44$
-	-	2.4853	5	643
2.484	20	2.4830	16	804
-	-	2.4626	4	260
-	-	2.4327	8	$\bar{2}61$
-	-	2.4315	5	$\bar{8}41$
-	-	2.4255	7	1021
-	-	2.3863	4	062
-	-	2.3726	5	$\bar{8}24$
-	-	2.2566	5	063
-	-	2.2423	8	445
-	-	2.0655	4	$\bar{1}042$
-	-	2.0283	5	$\bar{4}46$
-	-	2.0214	6	446
-	-	1.9604	4	$\bar{8}26$
-	-	1.8810	9	080
1.880	**30**	1.8781	27	$\bar{1}\bar{2}40$
-	-	1.8372	8	$\bar{8}07$
1.830	10	1.8291	14	447
-	-	1.6686	5	$\bar{4}47$
-	-	1.6110	8	$\bar{1}\bar{2}45$
-	-	1.6085	5	085
-	-	1.6024	7	$\bar{1}\bar{2}45$
-	-	1.5513	5	0010
-	-	1.5256	4	$\bar{4}49$

1 = observed diffraction pattern; 2 = calculated diffraction pattern obtained with the ferrofettelite structural model reported by Bindi *et al.* (2012) (only reflections with $I_{rel} \geq 4$ are listed). The strongest observed reflections are given in bold.

https://doi.org/10.1180/mgm.2022.28 Published online by Cambridge University Press

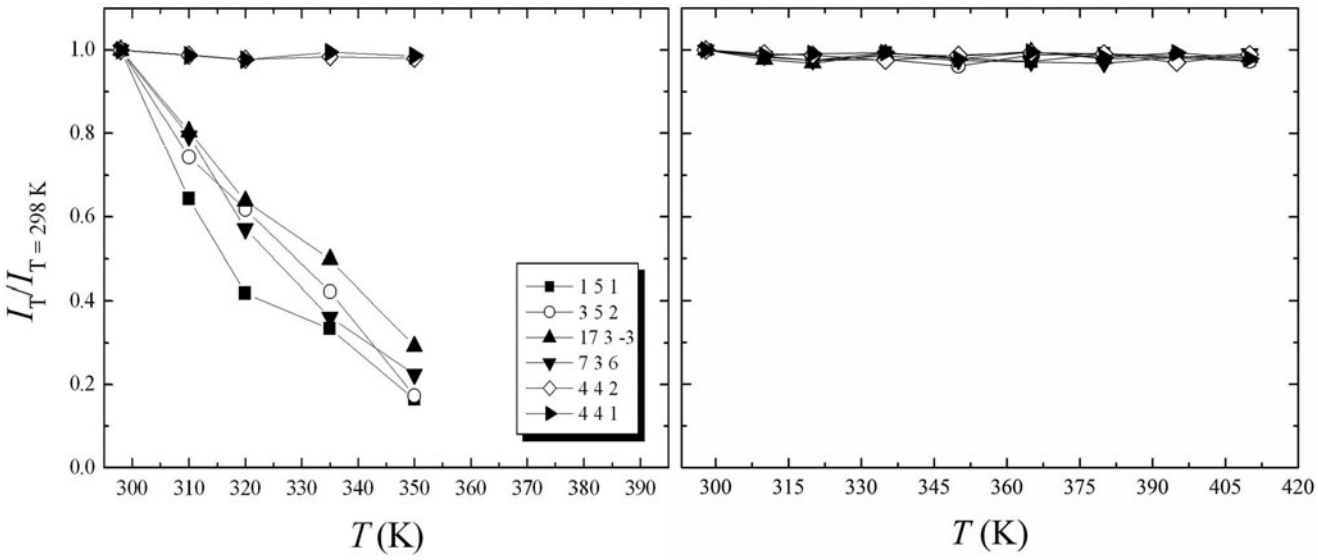

Fig. 2. Temperature dependence of the relative intensity of some selected reflections normalised to the value measured at 298 K. For fettelite (left) the intensity of reflections having h and $k = 2n + 1$ becomes very weak when the temperature increases whereas that of reflections having h and $k = 2n$ remains constant. In ferro-fettelite (right) the intensity of all the reflections remain constant.

Table 3. Unit-cell parameters for the selected ferrofettelite crystal at different temperatures.

T(K)	a (Å)	b (Å)	c (Å)	β (°)	V (Å^3)
298	26.011(2)	15.048(1)	15.513(1)	90.40(1)	6071.9(7)
310	26.072(3)	15.069(2)	15.535(2)	90.37(3)	6103.2(8)
320	26.135(4)	15.098(4)	15.557(3)	90.35(3)	6138.5(9)
335	26.193(4)	15.122(4)	15.566(4)	90.29(4)	6165(1)
350	26.244(5)	15.143(5)	15.589(5)	90.22(5)	6195(1)
365	26.281(6)	15.165(5)	15.612(5)	90.14(5)	6222(2)
380	26.312(7)	15.182(6)	15.630(6)	90.10(6)	6244(2)
395	26.344(8)	15.199(7)	15.647(7)	90.06(7)	6265(3)
410	26.381(9)	15.217(8)	15.672(8)	90.02(9)	6291(3)
335*	26.195(8)	15.125(8)	15.564(8)	90.24(8)	6166(4)

*Unit-cell parameters re-measured at 335 K after cooling.

polishing), the problem was solved, and we were able to obtain very good chemical data and in agreement with the chemical formula obtained from the structure refinement (Bindi *et al.*, 2012). The results of the analyses are given in Table 1.

The empirical formula (based on 36 apfu) can be written as $Ag_{16.04}(Fe_{0.55}Hg_{0.40}Cu_{0.02})_{\Sigma 0.97}(As_{3.94}Sb_{0.03})_{\Sigma 3.97}S_{15.02}$. The simplified formula is $Ag_{16}(Fe,Hg,Cu)(As,Sb)_4S_{15}$. The ideal formula, taking into account the structural results (see below and Bindi *et al.*, 2012) is, $[Ag_6As_2S_7][Ag_{10}FeAs_2S_8]$, which requires Ag 67.35, Fe 2.18, As 11.70, S 18.77, total 100 wt.%.

X-ray crystallography

The crystal structure refinement of ferrofettelite has been described in detail by Bindi *et al.* (2012) where the mineral was labelled R100124. At room temperature ferrofettelite is monoclinic (pseudo-hexagonal), space group $C2$, with $a = 26.011(2)$, $b = 15.048(1)$, $c = 15.513(1)$ Å, $\beta = 90.40(1)°$, $V = 6071.9(7)$ Å^3 and $Z = 8$ [$R = 0.0314$ for 8136 reflections with $I > 2\sigma(I)$]. The crystallographic information file has been deposited with the Principal Editor of *Mineralogical Magazine* and is available as Supplementary material (see below).

Powder X-ray diffraction data (Table 2) were obtained with an Oxford Diffraction Xcalibur PX Ultra diffractometer fitted with a 165 mm diagonal Onyx CCD detector and using copper radiation (Cu$K\alpha$, $\lambda = 1.54138$ Å). The working conditions were 50 kV, 50 mA and 3 hours of exposure; the detector-to-sample distance was 7 cm. The program *Crysalis* RED was used to convert the observed diffraction rings to a conventional powder diffraction pattern. Least squares refinement gave the following values: $a = 26.000(2)$, $b = 15.067(2)$, $c = 15.512(1)$ Å, $\beta = 90.29(1)°$ and $V = 6076.6(8)$ Å^3.

To compare the high-temperature behaviour of ferrofettelite with that of the Chilean fettelite (Bindi and Menchetti, 2011) the unit-cell values were carefully measured by means of an Oxford Diffraction Xcalibur 3 single-crystal diffractometer (enhanced X-ray source, X-ray radiation Mo$K\alpha$, $\lambda = 0.71073$ Å) fitted with a Sapphire 2 CCD detector. Moreover, in expectation of a possible phase transition towards a high-conducting form as for fettelite (Bindi and Menchetti, 2011), we monitored the intensities of some selected *hkl* reflections, i.e. 151, 352, 17$\bar{3}$, 736, 442 and 441, together with their equivalent reflections (Fig. 2). We chose four *hkl* reflections with h and $k = 2n+1$ to see if the a and b parameters became halved with the increase of temperature (see Bindi *et al.*, 2009), and two *hkl* reflections with h and $k = 2n$ (always present) as standard. Subsequently, the temperature was raised to 310 K with a heating rate of 5 K/h, and the same data set was collected. The same procedure was then repeated at 320, 335, 350, 365, 380, 395 and 410 K (Fig. 2). The high (up to 410 K) temperatures were achieved by means of an Oxford cryostream cooler. Unlike what was observed for fettelite, the intensities of the selected reflections with h and $k = 2n + 1$ (i.e. 151, 352, 17$\bar{3}$, 736) did not change in the temperature range investigated.

The unit-cell parameters obtained at the different temperatures are reported in Table 3. Before each measurement the sample was maintained at the specified temperature for ~20 min. As a check,

https://doi.org/10.1180/mgm.2022.28 Published online by Cambridge University Press

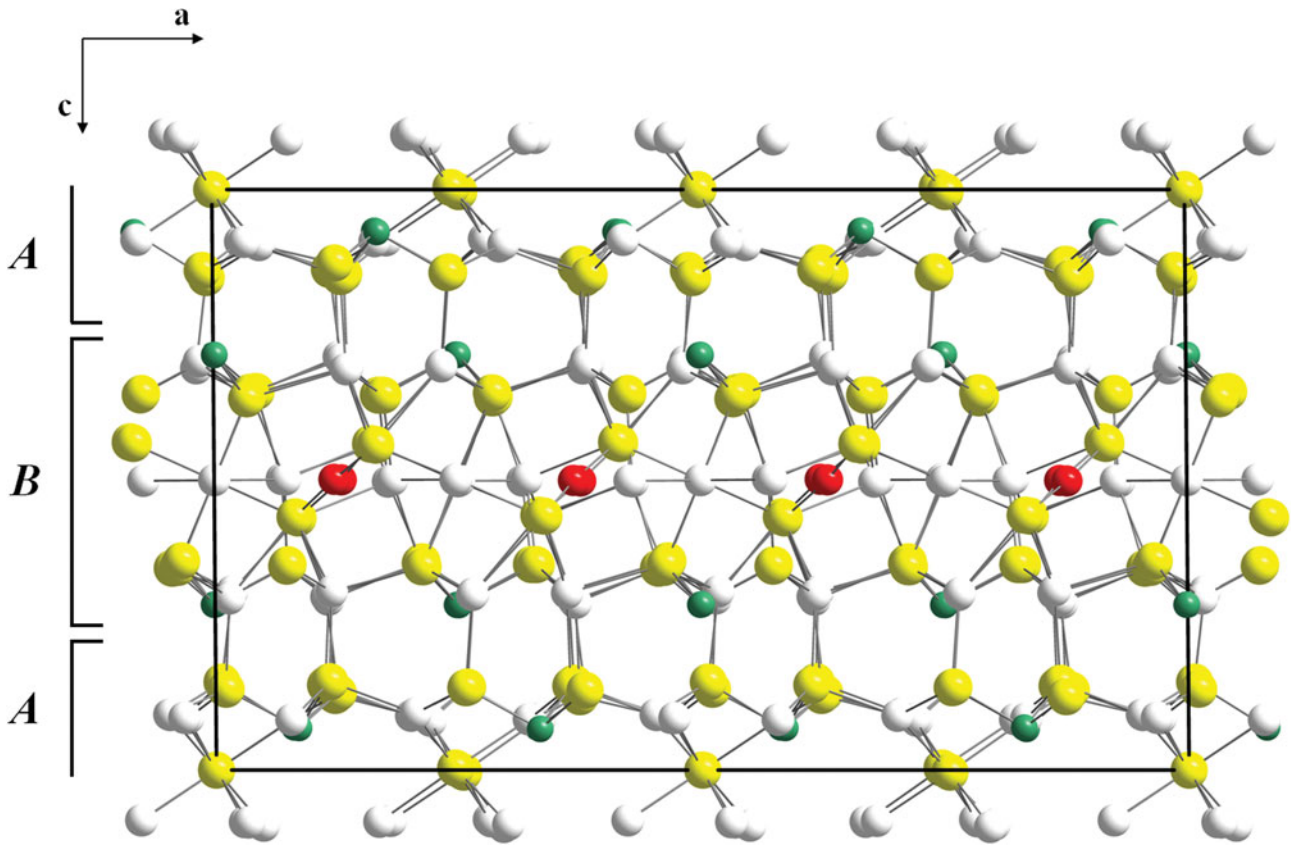

Fig. 3. Projection of the ferrofettelite structure along the monoclinic **b** axis, emphasizing the succession of the $[Ag_6As_2S_7]^{2-}$ *A* and $[Ag_{10}FeAs_2S_8]^{2+}$ *B* module layers. White, green, red and yellow circles indicate Ag, As, Fe and S atoms, respectively. The unit-cell and the orientation of the structure are outlined.

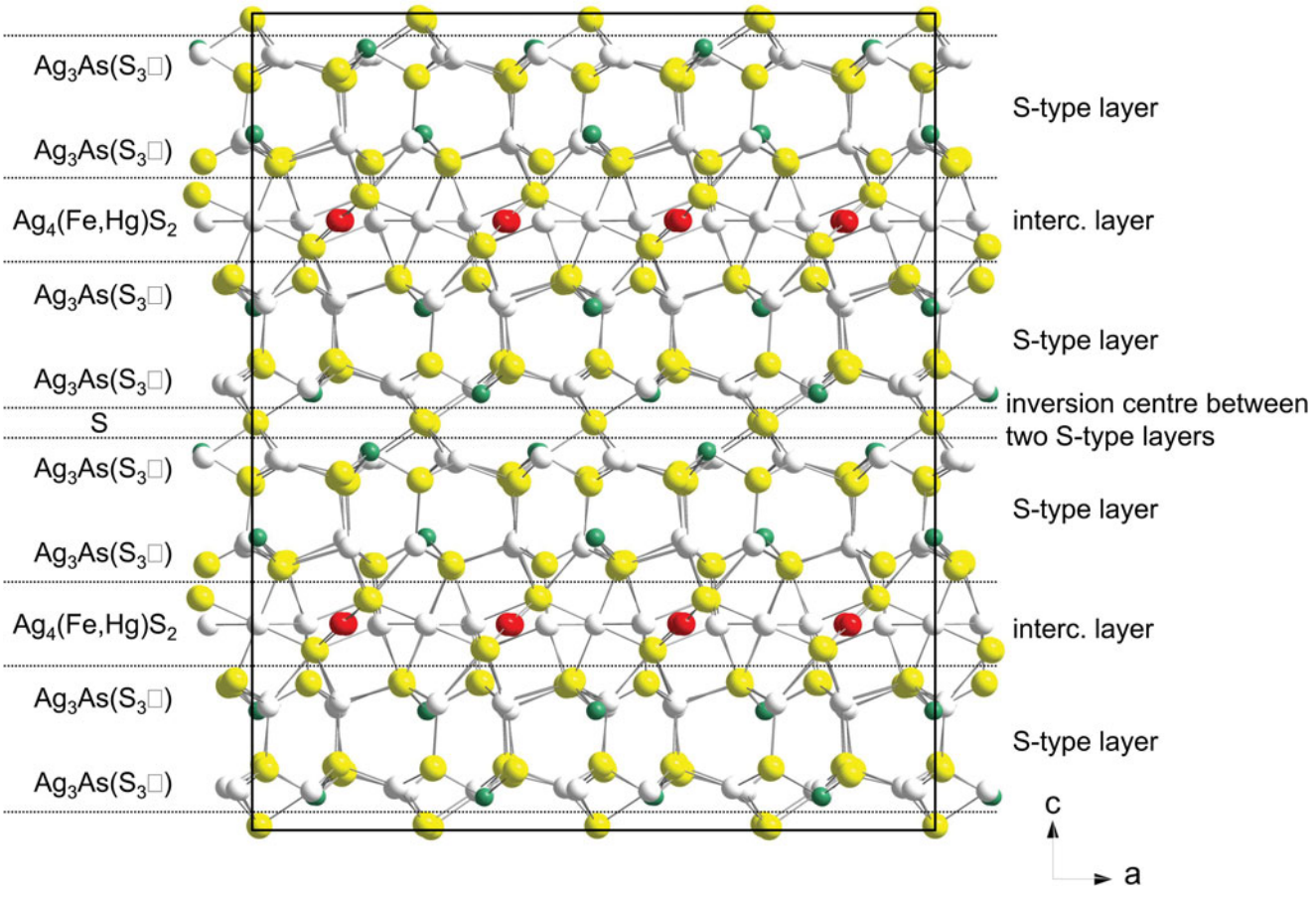

Fig. 4. Modular description of the crystal structure of ferrofettelite. 'S-type layer' stands for 'sphalerite-type layer' and 'interc. Layer' stands for 'intercalated $Ag_4(Fe,Hg)S_2$ layer'. See text for explanations. Symbols and orientation of the structure as in Fig. 3.

https://doi.org/10.1180/mgm.2022.28 Published online by Cambridge University Press

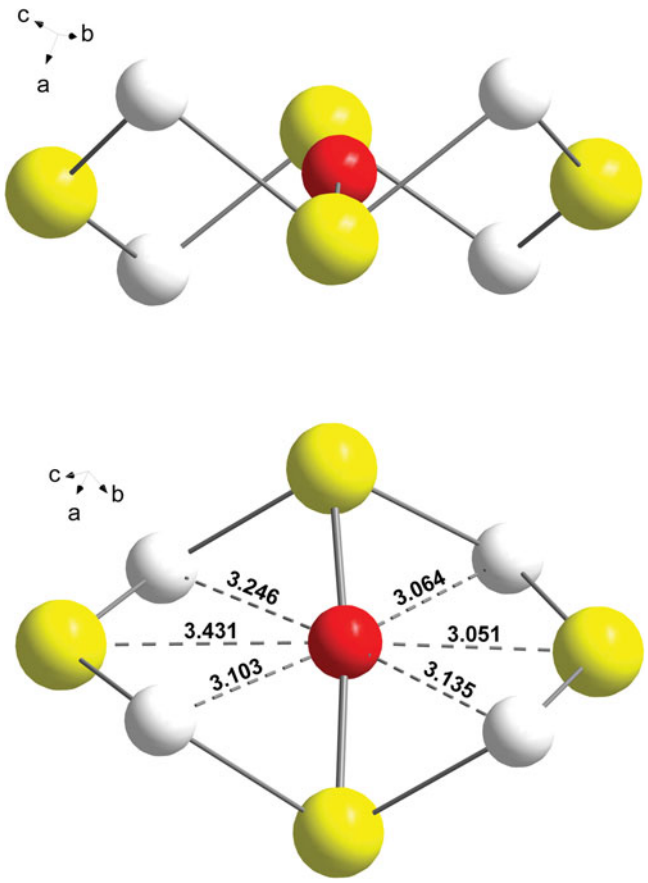

Fig. 5. A portion (at different orientations) of the crystal structure of ferrofettelite emphasising the Fe^{2+} coordination sphere. Short bond distances are depicted with a solid lines, long contacts with Ag and additional S atoms are given as dashed lines. The orientation of the structure is outlined. Symbols as in Fig. 3.

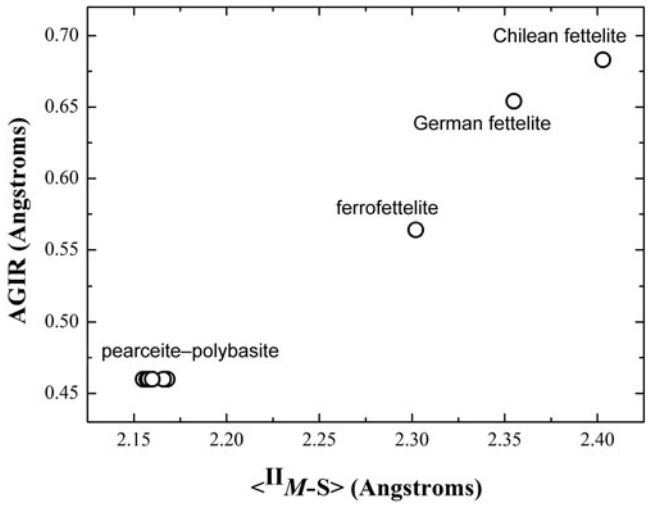

Fig. 6. Relationship between the $<^{II}M–S>$ distances (Å) versus the aggregated ionic radius (AGIR) (Å) for ferrofettelite (this study), German fettelite (Bindi *et al.*, 2012), Chilean fettelite (Bindi *et al.*, 2009) and minerals of the pearceite–polybasite group (Bindi *et al.*, 2006, 2007a, 2007b, 2007c, 2020; Evain *et al.*, 2006).

the crystal was cooled from 410 K to 335 K. The unit-cell values obtained did not reveal significant variations from the previous one, thus indicating that no hysteresis occurs within the temperature range examined.

Discussion

Crystal-chemical considerations

As already reported by Bindi *et al.* (2012), the crystal structure of ferrofettelite is nearly identical to that reported previously by Bindi *et al.* (2009) for fettelite. In brief, the structure can be described as the alternation of two kinds of layers along the **c**-axis (Fig. 3): layer *A* with general composition $[Ag_6As_2S_7]^{2-}$ (almost identical to that found in the structure of pearceite–polybasite group of minerals; Bindi *et al.*, 2020) and layer *B* with a general composition of $[Ag_{10}FeAs_2S_8]^{2+}$. In the structure, the Ag atoms adopt various coordinations extending from quasi linear to quasi tetrahedral, the AsS_3 groups form pyramids as are typically observed in sulfosalts, and Fe links two sulfur atoms in a linear coordination with mean bond distances of 2.302 and 2.310 Å.

Alternatively, the ferrofettelite structure can be described as based on *two-atom-thick* Ag-enargite-type layers with one S vacancy [i.e. $Ag_3As(S_3\square)$] (which correspond to pseudo-hexagonal sphalerite-type layers), and an intercalation of *a single* one-atom-thick $Ag_4(Fe,Hg)S_2$ layer (Fig. 4). The (Fe,Hg) atom can be considered as a 'bridging cation'. The connection between two unit-cells along **c** is possible with an isolated S atom that acts as inversion centre between two sphalerite-type layers. With this approach, the resulting general formula could be written as $[Ag_3As(S_3\square)]_2+(S)+[Ag_3As(S_3\square)]_2+[Ag_4(Fe,Hg)S_2]$, which corresponds to $(Ag_{12}As_4S_{12})S[Ag_4(Fe,Hg)S_2]$. Using this modular description, the pearceite–polybasite structure (Bindi *et al.*, 2020) could be envisioned as composed by two *one-atom-thick* Ag-enargite-type layers together with two *one-atom-thick* 'pure' Ag layers.

The structural positions of the *B* module layer hosting Fe in ferrofettelite are not fully occupied by Fe but can be written as $Fe_{0.57}Hg_{0.41}Cu_{0.02}$ (by normalising the population of the site to 1.00). The $Fe^{2+} \leftrightarrow Hg$ substitution is supported by the decrease in the mean bond distances with respect to the fully occupied Hg positions in fettelite, i.e. 2.393 and 2.403 Å, respectively (Bindi *et al.*, 2009).

A very interesting and peculiar feature in the ferrofettelite structure is the linearly coordinated Fe^{2+} cation. Even if it is not a fully Fe^{2+}-occupied site, to the best of our knowledge, this is the first inorganic compound having $^{II}Fe^{2+}$ (as a dominant cation) ever reported. Fe^{2+} coordinates linearly two sulfur atoms and is hosted in a cavity with four Ag atoms at distances in the range 3.064–3.246 Å and two additional sulfur atoms at distances of 3.051 and 3.431 Å (Fig. 5). There are examples of linearly coordinated Fe^{2+} with oxygen in complex organic compounds (e.g. Reiff *et al.*, 2009) or examples of organic complexes with linearly-coordinated monovalent iron with N and C (e.g. Zadrozny *et al.*, 2013), but no previously reported examples in inorganic crystal structures. It is very likely that the linear coordination is favoured by the presence of large amounts of Hg at the same sites. Nevertheless, given the importance of Fe^{2+} in two-fold coordination with S, we have tried to estimate its ionic radius. By plotting the two mean bond distances of the linearly coordinated sites – including also a Cu-enriched fettelite from Germany studied by Bindi *et al.* (2012) exhibiting a chemistry of the (Hg,Cu,Fe) site of $Hg_{0.84}Cu_{0.15}Fe_{0.01}$ and having mean

https://doi.org/10.1180/mgm.2022.28 Published online by Cambridge University Press

bond distances of 2.335 and 2.355 Å, and selected members of the pearceite–polybasite group of minerals having Cu sites (Bindi *et al.*, 2006, 2007a, 2007b, 2007c; Evain *et al.*, 2006) – against the aggregated ionic radius (i.e. AGIR), we assessed a value for the ionic radius of Fe^{2+} in two-fold coordination of ~0.50 Å (Fig. 6). A similar value can be obtained by considering the unit-cell volume of the three samples [ferrofettelite: 6071.9 $Å^3$ (this study), Cu-bearing fettelite: 6085.0 $Å^3$ (Bindi *et al.*, 2012) and fettelite: 6095.2 $Å^3$ (Bindi *et al.*, 2009)] as a function of the AGIR. Interestingly, a recent machine learning approach carried out to extend the Shannon's ionic radii database (Baloch *et al.*, 2021) reported a value of 0.478 Å for $^{II}Fe^{2+}$, in excellent agreement with that inferred from our crystal-chemical lucubrations.

High-temperature behaviour

Bindi and Menchetti (2011) found that fettelite undergoes an ionic phase transition at ~380 K. In the high-temperature structure, the *A* module layer is identical to that at room temperature. On the contrary, in the *B* module layer silver atoms are distributed along a diffusion path thus leading to a quasi-liquid displacement for these ions. This is characteristic of superionic conductors that show a strong disorder in the sub-lattice of the moving cations. As is evident from Fig. 2, ferrofettelite does not undergo any phase transition. It is not clear at the moment why Fe atoms (the only difference with respect to pure fettelite) inhibits the fast-ion conduction. Although it is well known that Hg is more mobile than Fe in ionic conductors, it is hard to think that the presence of iron dominating over Hg in the linear sites can be the only responsible feature. Further experimental work at temperature higher than 410 K will be carried to shed light on the structural behaviour of ferrofettelite.

Supplementary material. To view supplementary material for this article, please visit https://doi.org/10.1180/mgm.2022.28

Acknowledgements. We wish to thank Frantisek Laufek, Yves Moëlo, Stuart Mills and Oleg Siidra for their helpful comments. This research received support by Ministero dell'Istruzione, dell'Università e della Ricerca through the project PRIN 2017 "TEOREM – deciphering geological processes using Terrestrial and Extraterrestrial ORE Minerals", prot. 2017AK8C32 (PI: Luca Bindi).

References

Baloch A.A.B., Alqahtani S.M., Mumtaz F., Muqaibel A.H., Rashkeev. S.N. and Alharbi F.H. (2021) Extending Shannon's ionic radii database using machine learning. *Physical Review Materials*, **5**, 043804.

Bindi L. and Downs R.T. (2022) Ferrofettelite, IMA 2021-094. CNMNC Newsletter 65; *Mineralogical Magazine*, **86**, https://doi.org/10.1180/mgm.2022.14

Bindi L. and Menchetti S. (2011) Fast ion conduction character and ionic phase-transition in silver sulfosalts: The case of fettelite [$Ag_6As_2S_7$][$Ag_{10}HgAs_2S_8$]. *American Mineralogist*, **96**, 792–796.

Bindi L., Evain M. and Menchetti S. (2006) Temperature dependence of the silver distribution in the crystal structure of natural pearceite, $(Ag,Cu)_{16}(As,Sb)_2S_{11}$. *Acta Crystallographica,* **B62**, 212–219.

Bindi L., Evain M., Spry P.G. and Menchetti S. (2007a) The pearceite-polybasite group of minerals: Crystal chemistry and new nomenclature rules. *American Mineralogist*, **92**, 918–925.

Bindi L., Evain M. and Menchetti S. (2007b) Complex twinning, polytypism and disorder phenomena in the crystal structures of antimonpearceite and arsenpolybasite. *The Canadian Mineralogist*, **45**, 321–333.

Bindi L., Evain M., Spry P.G., Tait K.T. and Menchetti S. (2007c) Structural role of copper in the minerals of the pearceite-polybasite group: The case of the new minerals cupropearceite and cupropolybasite. *Mineralogical Magazine*, **71**, 641–650.

Bindi L., Keutsch F.N., Francis C.A. and Menchetti S. (2009) Fettelite, [$Ag_6As_2S_7$][$Ag_{10}HgAs_2S_8$] from Chañarcillo, Chile: Crystal structure, pseudosymmetry, twinning, and revised chemical formula. *American Mineralogist*, **94**, 609–615.

Bindi L., Downs R.T., Spry P.G., Pinch W.W. and Menchetti S. (2012) A chemical and structural re-examination of fettelite samples from the type locality, Odenwald, southwest Germany. *Mineralogical Magazine*, **76**, 551–566.

Bindi L., Nespolo M., Krivovichev S., Chapuis G. and Biagioni C. (2020) Producing highly complicated materials. Nature does it better. *Reports on Progress in Physics*, **83**, 106501.

Evain M., Bindi L. and Menchetti S. (2006) Structural complexity in minerals: twinning, polytypism and disorder in the crystal structure of polybasite, $(Ag,Cu)_{16}(Sb,As)_2S_{11}$. *Acta Crystallographica,* **B62**, 447–456.

Reiff W.M., Schulz C.E., Whangbo M.-H., Seo J.I., Lee Y.S., Potratz G.R., Spicer C.W. and Girolami G.S. (2009) Consequences of a linear two-coordinate geometry for the orbital magnetism and jahn−teller distortion behavior of the high spin iron(II) complex $Fe[N(t\text{-}Bu)_2]_2$. *Journal of American Chemical Society*, **131**, 404–405.

Wang N. and Paniagua A. (1996) Fettelite, a new Hg-sulfosalt mineral from Odenwald. *Neues Jahrbuch für Mineralogie Monatshefte*, **1996**, 313–320.

Zadrozny J., Xiao D., Atanasov M., Long G.J., Grandjean F., Neese F. and Long J.R. (2013) Magnetic blocking in a linear iron(I) complex. *Nature Chemistry*, **5**, 577–581.